Attractive Force of the Magnetic Attachment Using Three-Dimensional Finite Element Method -An Influence of Magnetic Circuit-

H. Kumano, Y. Nakamura, H. Nagai, R. Kanbara, T. Masuda, K. Hayashi, Y. Takada[1], Y. Ohno, Y. Tanaka

Department of Removable Prosthodontics, School of Dentistry, Aichi-Gakuin University
[1]Division of Dental Biomaterials, Tohoku University Graduate School of Dentistry

Introduction

The functional retention of dental magnetic attachments is based upon the simple physics of magnetic attractive force. Permanent magnets used as early dental magnetic attachments were first introduced in early 1950's, and were applied in different mechanical applications and clinical uses. Magnet implantation to the jaws[1)], and an opposing use of magnetic repulsion[2)] are two main examples. Various magnetic attachments designs of significant design have since been developed. As stainless steel micro laser welding technology became available in the 1990's, corrosion resistance was improved by the protective stainless steel encasement covering. These newer encased magnets provided improved corrosion resistance and improved magnetic attachment retention and clinical durability. As newer magnetic materials have been developed, the advantages of size reduction, stronger attractive retentive force, and improved clinical utility and use have substantially improved the range of useful applications compared to earlier versions previously available.

While certain types of esthetically hidden precision attachments are considered rigid and inflexible, magnetic attachments are considered more capable of stress release due to an inherent ability to minimize and reduce unfavorable horizontal mechanical force transfer. Reduced horizontal force transfer for prosthetic retentive elements has been considered advantageous in preventing abutment overload and unwanted breakdown. A smaller attachment size is also of greater benefit for esthetic adaptability and constrained space applications. [3-5)].

Different designs of keeper and magnetic assembly have been developed to reduce attachment size and provide optimum attractive force for useful retention. Different designs have been shown to vary in magnetic circuit and retention strength. An ideal design will have an optimal magnetic circuit, providing for the development of a magnetic attachment assembly of high retentive value for clinical application while maintaining a minimal profile requirement.

Finite element analysis has been considered an effective means of magnetic circuit evaluation for the evaluation of design parameters. The finite element method permits qualitative visualization the physical dynamics of the magnets tested while also rendering quantitative values useful for comparative evaluation of different designs and conditions. Objective

Repeated load was applied on a keeper of the implant to investigate loosening at the junction between a keeper and abutment during function.

Materials and Methods

1. Analysis model

A proprietary dental magnet design was selected as an analysis sample for component configuration testing (GIGAUSS D600, GC.) The dimensional shape and size of the test sample dental magnet were measured prior to modeling procedures. Comparative measurements of the outer surface structures of the attachment were obtained for comparison of manufacturer specifications and actual values obtained.

The inner structure of the magnetic attachment was evaluated by embedment sectioning and evaluation. The magnetic assembly was embedded with embedding agent (SCANDIQUICK, SCANDIA) and sectioned using an automatic precision cutter (Isomet, BUELER). The resulting sections were evaluated and measured using a surface shape measurement apparatus (VF-7510, KEYENCE).

The analysis model was constructed based on the measurements obtained. The size of a magnetic assembly was 3.6 mm in diameter and 1.3 mm in height, and the inner magnetic assembly was determined to be a round-shape with 2.2 mm diameter and 0.5 mm height dimensions. The size of the shield ring was 0.2 mm in width and its height was 0.2 mm. (Fig. 1).

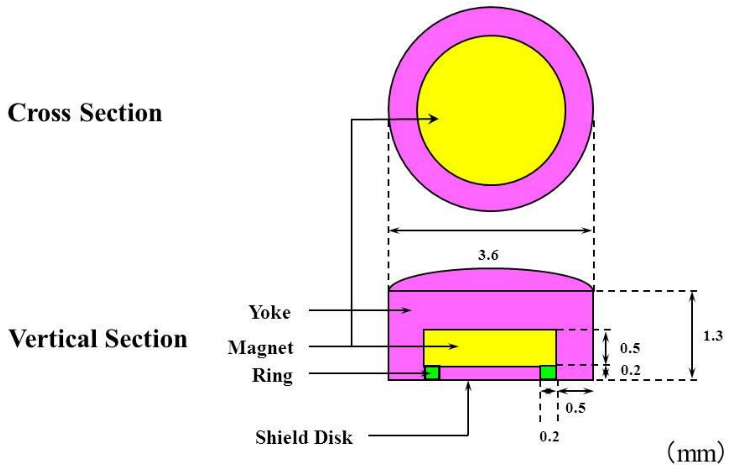

Fig1 : Size of the magnetic attachment

The shield disc components of the magnetic assembly were fabricated using a non-magnetic material as the analysis object. The diameter of a non-magnetic material was incrementally thickened by 0.1 mm to 2.0 mm maximum thickness for each of the 21 modeling test samples prepared (Fig. 2).

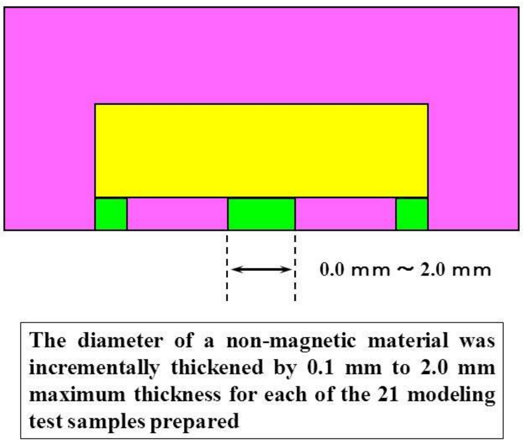

Fig2 : Analysis items

Each model was fabricated as a one fourth size model. The model were designed to be axially symmetric. The defined scope of FEM analysis range was set as 2 mm around a keeper and magnetic assembly.

The models were constructed using a general purpose finite element pre-/post-processor (Femap USG) and an electromagnetic field analysis system (μ-MF analysis software). The shaping elements were defined by three-dimensional pentahedron and hexahedron elements. The element count was 53,802, and the nodal points number was 57,784 (Fig. 3).

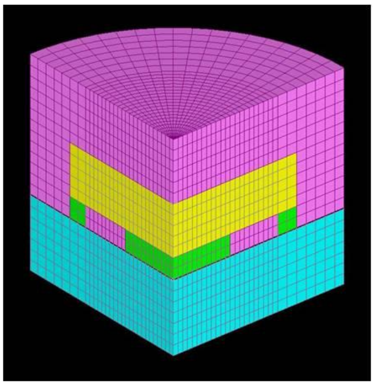

Element type	:	**three-dimensional Pentahedron and hexahedron elements**
Elements	:	**53,802**
Nodes	:	**57,784**

Fig3 : Analysis model

2. Analysis conditions

The magnetic property was determined based on previously obtained the thermal property data for the GIGAUSS D600 magnetic attachment[6] and the manufacture's reported thermal property data values. Although the material of a yoke and keeper was SUSXM27, the magnetic property details are undisclosed. An extrapolated value was thus selected. The extrapolated value used SUS447J1 material values, and was utilized to approximate the B-H curve. The approximated curve was used for the finite element magnetic material property values. (Table 1) Analysis results were then obtained for magnetic flex density distribution and attractive force.

Table1 : Analysis conditions

- **Component**
  - Magnetic assembly — Magnet : Nd-Fe-B; Yoke : SUS447J1
  - Keeper : SUS447J1
- **Magnetic Characteristic**
  - Magnet — (BH) max = 46 MGOe; Residual magnetic induction = 1.22 T
  - Yoke — Saturation magnetic induction = 1.35 T

B-H curve $B = Bs \{ 1 - \exp (-\mu_r \cdot \mu_0 \cdot H / Bs) \}$

Results

1. Magnetic flux density distribution

Fig. 4 shows the magnetic flux density distribution of the analysis results. The magnetic flux density distribution of the magnetic assembly and the attractive surface of a keeper demonstrate increase as the diameter of a non-magnetic material increases. However, as the diameter of non-magnetic material became greater than 0.6 mm, the areas of the oversaturated magnetic flux density field were observed within the shield disk. As the diameter of a non-magnetic material increased further, the interior areas of the shield disk became completely oversaturated with the magnetic flux density and the overall magnetic flux distribution within the magnetic assembly decreased.

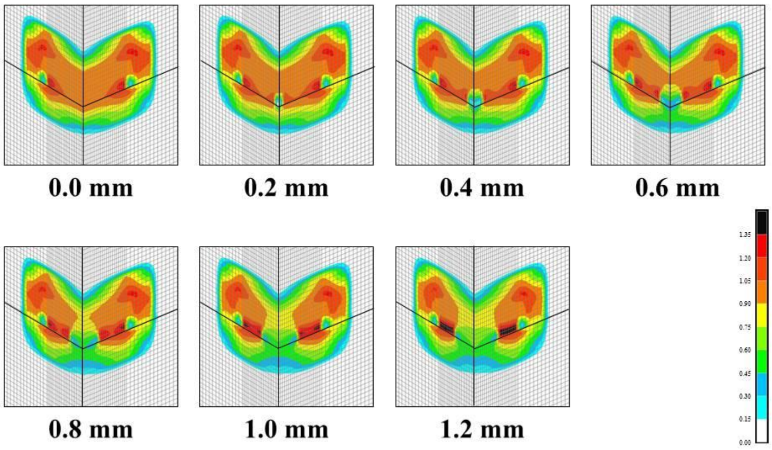

Fig4 : Magnetic flux density distribution

2. Attractive force

Fig. 5, records the attractive force analysis results. Attractive force moderately increased to 540 g until the diameter of a non-magnetic material became 0.5 mm, and decreased with further increasing diameter. When the attractive force of a non-magnetic material with 0.0 mm diameter was considered as 100%, attractive force peaked to 103% at 0.5 mm in diameter, decreased to 100% at 0.7 mm in diameter, and 86% at 1.2 m in diameter.

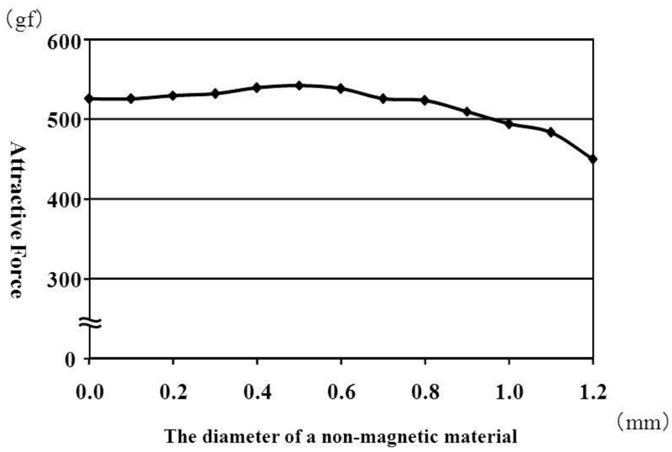

Fig5 : Attractive Force

Discussion

Although direct measurement of a magnetic force and field is possible, it is extremely difficult to design a magnet that exerts the maximum magnetic force based on the measurement results, without verifying an optimization for minimum magnetic field leakage. The present study performed a magnetic field analysis using the 3D Finite Element Method.

As magnetic field distribution occurs in space, the space around the analysis model and integration path on the interface between a magnet assembly and keeper should be properly contained and subdivided. Preliminary analysis was performed and calculated optimal shield thickness values with minimal negative influence, suggesting high analysis accuracy of the present study.

Although the specific magnetic properties of a magnetic stainless steel and magnet are important analysis conditions, little is known about these individual properties. To solve the problem, the value of SUS447J1, which is considered to have the close approximation magnetic properties based on formulation content as SUSXM27, was substituted to approximate the B-H curve for the study analysis. Accurate measurement of these values, and a continued search for better magnetic property materials are true challenges for the future.

The attractive force of a magnet is defined as $F = (1/2\ \mu_0)\cdot S\cdot B^2$ {μ_0: space permeability, S: attractive surface area, B: magnetic flux density}. This formula shows that attractive force is proportional to the magnetic flux density and attractive magnetic surface. Magnetic flux density is a magnetic flux flow per unit area, and shows the magnetic strength. Magnetic flux density increases with an increase of external magnetic field. The ratio between the magnetic flux density and magnetic field is called magnetic permeability, and higher magnetic flux density can be obtained in higher magnetic permeability even in a weak magnetic field. Since an external magnetic field was not applied in the present study, the magnetic permeability is constant. Therefore, attractive force of a magnet increases with an increase of magnetic flux density. Moreover, the magnetic flux density reaches a limit when magnetic field is added to magnetic material. This is called saturated magnetic flux density, and as magnetic flux density becomes oversaturated, it decreases as it exceeds this inversion point.

In the present study, the magnetic flux density within a magnetic assembly was significantly altered by changing the diametric thickness of a non-magnetic shield material. Magnetic flux density within the magnetic assembly became saturated when the diameter of a non-magnetic material exceeded a 0.5 mm threshold. Attractive force is therefore shown to be influenced by a magnetic flux density increase rather than by a simple decrease of magnetic attractive surface area. Exceeding the threshold diameter of a non-magnetic material resulted decreased magnetic flux density and decreased attractive surface area, lowering the resulting attractive force. Further analysis is required to obtain information and optimized magnetic attachments.

Conclusion

A non-magnetic material was designed at the center of a shield disk of a magnetic assembly of a dental magnetic attachment. The influence of magnetic circuit was analyzed and evaluated using a three-dimensional finite element method, and the following results were obtained.

1. Attractive force increased until the diameter of a non-magnetic material in the shield disk became 0.5 mm. A peak attractive force was approximately 540 gf at 0.5 mm diameter. When the attractive force of a non-magnetic material with 0.0 mm diameter was considered as 100%, a peak attractive force was 103%.
2. Attractive force started decreasing when the diameter of a non-magnetic material in the shield disk exceeded 0.5 mm. Attractive force decreased to 86% when the diameter of a non-magnetic material was 1.2 mm.

References

1. Behrman SJ.: The implantation of magnets in the jaw to aid denture retention, J Prosth Dent 10 : 807-841,1960
2. Freedman H.: Magnets to stsbilize dentures, JADA 47 : 288-343,1953
3. Tanaka Y.: Magnetic Attachment –New Prosthetic Treatment using magnets- Ishiyaku Publishers, Inc., 3-205, 1992
4. Tanaka Y.: Magnetic Attachment II -108 questions and answers- Ishiyaku Publishers, Inc, 2-159, 1995
5. Nakamura Y.: Stress analysis of overlay denture and a magnetic attachment using finite element method, J Jpn Prosthodont Soc,42: 234-245, 1998
6. Miyata T. Niimi J. And A. and et al: Infuluence of heating of a magnetic attachment on the attractive force, J J Mag Dent, 17(2): 44-50, 2008